Progress In Electromagnetics Research Letters, Vol. 109, 85–92, 2023

A Novel Planar Broadband End-Fire Antenna with High Front-to-Back Ratio

Yonghao Zhu, Hua Chen*, Lan Li, Jifang Zhang, Yan Yan, Mankang Xue, Quan Wang, and Qing Fang

Abstract—In this paper, a high front-to-back ratio (FTBR), broad bandwidth planar printing structure and electromagnetic dipole complementary antenna that generates end-fire radiation pattern is investigated. The antenna consists of a segmented loop, planar electric dipole, and microstrip coupling feed structure, which are printed on the top and bottom surfaces of a dielectric substrate. The segmented loop is equivalent to a magnetic dipole. A high front-to-back ratio is achieved by combining the electric dipole and equivalent magnetic dipole with the same radiation intensity and antiphase. The proposed antenna is fabricated and measured. The measured results show that the proposed antenna achieves an impedance bandwidth of 48.05% (1.66 GHz–2.71 GHz). The largest gain can get to 3.89 dBi, and the maximum front-to-back ratio is 25.4 dB in the frequency band. The measured results are well consistent with simulated ones.

1. INTRODUCTION

With the development of wireless communication technology, there is a higher demand for antenna miniaturization, anti-interference ability, etc. To the best of our knowledge, end-fire antennas with directional radiation patterns have better anti-interference ability which can suppress external interference in specified radiation direction [1]. In addition, with the miniaturization of the device design, the space left for the antenna is getting smaller. An end-fire antenna that can achieve directional radiation performance without an additional reflector has a broader range of applications [2, 3]. Hence, many end-fire antennas have been suggested, such as Quasi-Yagi antennas [4–7], dielectric resonator antennas [8, 9], and complementary antennas [10–12]. Quasi-Yagi antennas generally use driving elements and coupling reflectors, and some of them also need to add a reflection plate to ensure directionality, resulting in a large area occupied. Dielectric resonators have good end-fire characteristics, but they are three-dimensional structures, and they are not suitable in some limited space scenarios. In contrast, the complementary planar end-fire antenna composed of electric dipole and magnetic dipole has the advantages of low back radiation, low cost, low profile, and easy fabrication. On the other hand, a high front-to-back ratio antenna has a strong anti-interference ability, which can reduce the influence of interference in the system [13–17].

2. ANTENNA CONFIGURATION

Electromagnetic dipole complementary antenna possesses the admirable advantage of low back radiation [18–20]. The E-plane pattern of the electric dipole is the same as the H-plane pattern of the magnetic dipole, and the H-plane pattern is the same as the E-plane pattern of the magnetic dipole. When the spatial positions of an electric dipole and magnetic dipole are placed orthogonally,

Received 26 December 2022, Accepted 23 February 2023, Scheduled 7 March 2023
* Corresponding author: Hua Chen (cherrychen40600@163.com).
The authors are with the Kunming University of Science and Technology, Kunming 650500, China.

the excitation amplitude will be equal, and the phase difference will be 180° [21–23]. However, no single magnetic dipole has been found in nature, so the realization of magnetic dipole mostly adopts equivalence.

The configuration of the proposed planar end-fire antenna is shown in Fig. 1. The antenna mainly consists of three parts: a printed dipole, a segmented loop, and a microstrip coupling feed structure. The printed dipole is placed on the lower surface of the substrate, and the segmented loop is printed on the upper surface of the dielectric substrate. For the purpose of no additional size increase, the loop is placed around the feed structure. The stepped feed structure is used to adjust the impedance matching of the antenna. The optimal parameters of the antenna are listed in Table 1.

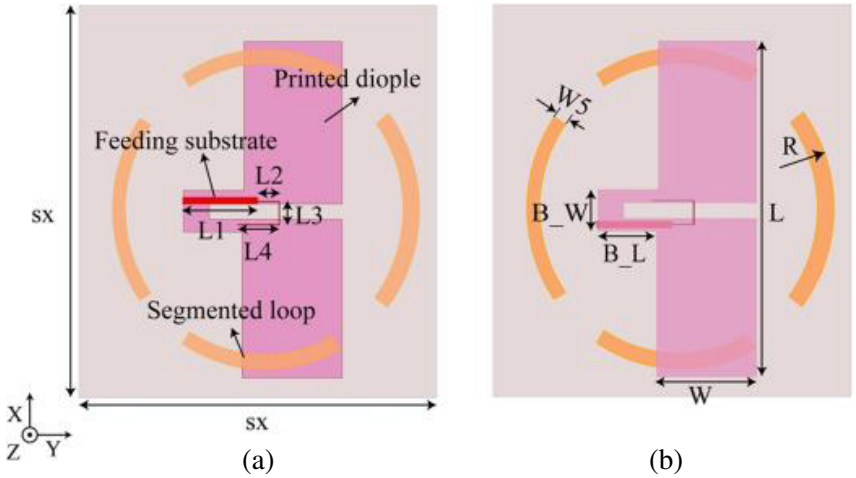

Figure 1. Configuration of the proposed antenna. (a) Top view. (b) Back view.

Table 1. Some dimensions of proposed antenna.

Parameter	Value mm	Parameter	Value mm
sx	78	$W5$	0.8
L	70	R	32
W	23.3	Lam	125
$L1$	16.3	$L2$	7.3
$L3$	5.1	$L4$	11.8
B_W	9	B_L	13

The designed antenna evolution process is shown in Fig. 2. At first, the dipole is printed on the bottom of the dielectric substrate, and the microstrip coupling feed is placed on the top, marked as Ant1. Since it is a single dipole, the front-to-back ratio of Ant1 in Fig. 3 is not ideal. To realize the magnetic dipole radiation, the continuous loop is printed on the dielectric substrate, marked as Ant2. However, this structure does not produce a current loop, and in Fig. 3, Ant2 has an improved front-to-back ratio between 2.5 and 2.6 GHz compared to Ant1, but still, no high front-to-back ratio is observed. Therefore, the antenna structure is further improved by truncating the continuous loop into four equal annular sectors and optimizing the radius and spatial location of the rings, marked as Ant3. The discontinuous ring at the top of the dielectric substrate is equivalent to a magnetic dipole, which forms an electromagnetic dipole complementary antenna with the printed dipole at the bottom, showing an excellent high front-to-back ratio in Ant3 in Fig. 3.

As shown in Fig. 4, it can be seen that the front-to-back ratio moves left with the radius increasing. On the one hand, as the radiator of the equivalent magnetic dipole, the radius of the discontinuous

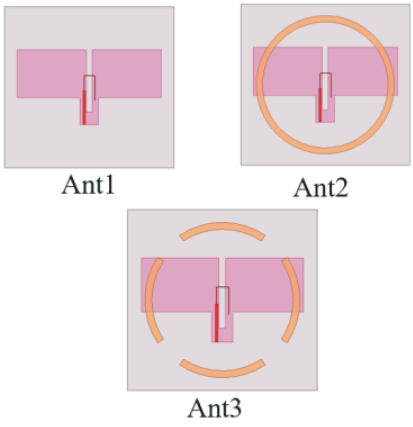

Figure 2. Antenna evolution process.

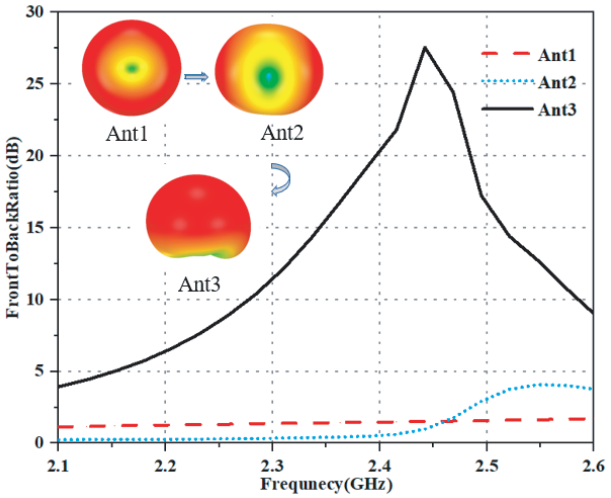

Figure 3. Front-to-back ratio in dB for the proposed antenna at different design steps.

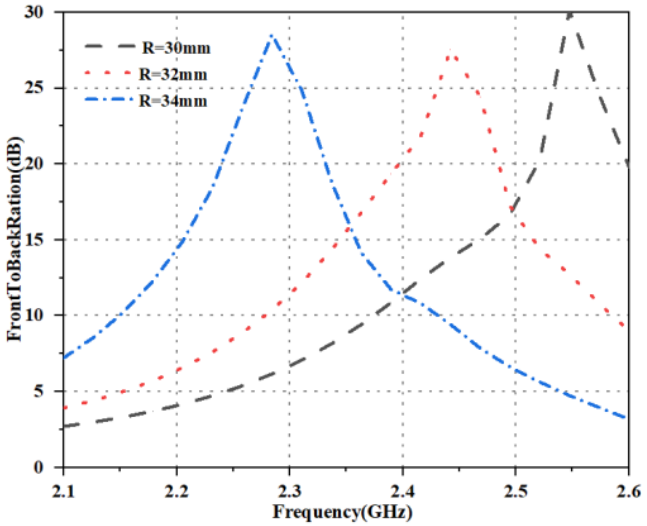

Figure 4. Influence of ring radius on front-to-back ratio.

ring determines the working frequency of the equivalent magnetic dipole. On the other hand, the phase difference between the equivalent magnetic dipole and electric dipole also affects the radiation characteristics of the antenna.

The final design of the proposed end-fire antenna is illustrated in Fig. 1. Fig. 5 shows the current density distributions of the proposed antenna at different time points (phases). Assuming that "T" is the current period, at initial time which is remarked as $t = 0$, the surface current of the printed dipole points to the x-direction, whereas it becomes divergent at $t = T/4$. When $t = T/2$, the surface current also points to the x-direction, the same as $t = 0$, whereas it becomes divergent at $t = 3T/4$, the same as $t = T/4$. When $t = T/4$, the segmented loop current reaches a maximum, while $t = 3T/4$, the same as $t = T/4$. Hence, it is shown that there exists a 90° phase difference between the printed dipole current and the segmented loop. There is also an inherent 90° phase difference between the current loop and the equivalent magnetic dipole [24]. As a result, 180° phase difference is informed between the equivalent magnetic dipole and an electric dipole, which meets the phase difference conditions of complementary antennas.

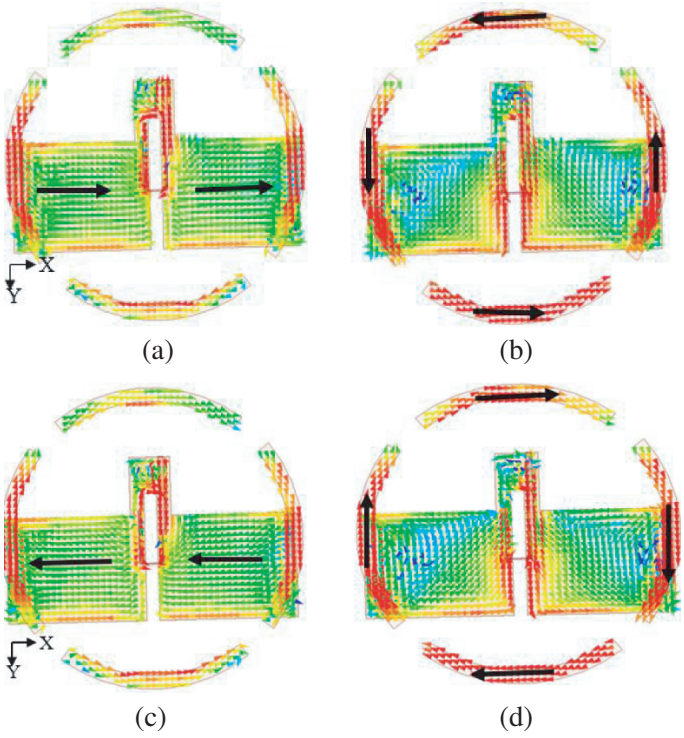

Figure 5. Simulated surface current distributions of the proposed antenna at different time points. (a) $t = 0$. (b) $t = T/4$. (c) $t = T/2$. (d) $t = 3T/4$.

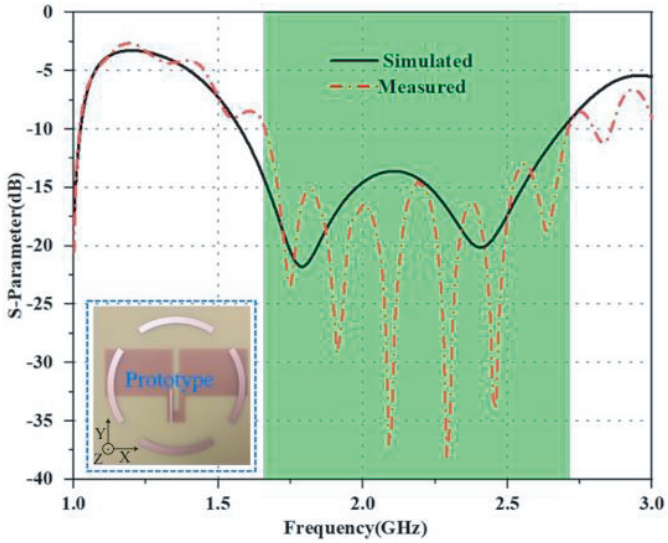

Figure 6. Measured and simulated S-parameter.

3. RESULTS AND DISCUSSIONS

Figure 6 shows the measured return loss of the proposed antenna. It can be seen from the figure that the return loss below -10 dB is achieved from 1.66 to 2.71 GHz. And the relative impedance bandwidth is about 48.05%. The small discrepancy is mainly due to the imperfection of fabrication and measurement.

Figure 7 shows the measured scenario of the antenna in an anechoic chamber. Data are provided by institutions. The simulated and measured x-y and y-z plane radiation patterns of the proposed antenna

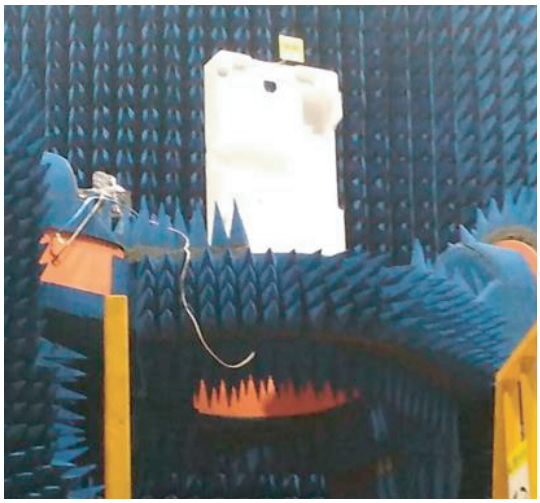

Figure 7. Anechoic chamber test diagram.

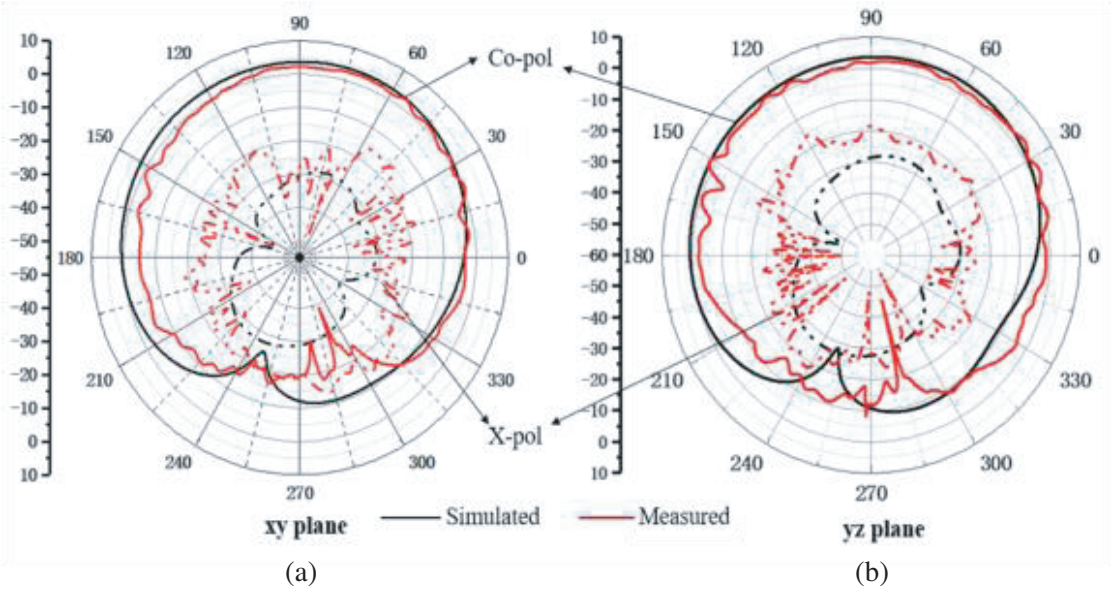

Figure 8. Simulated and measured radiation pattern of Co-polarization and X-polarization at 2.4 GHz. (a) x-y plane. (b) y-z plane.

at 2.4 GHz are shown in Fig. 8. The measured co-polarization patterns are slightly different from the simulated pattern. However, it is a normal phenomenon within the error range. The 3 dB beamwidths in x-y and y-z planes are about 145° and 150°. The measured and simulated front-to-back ratios are shown in Fig. 9. A peak front-to-back ratio value of 25.4 dB is achieved.

Figure 10 shows the measured and simulated results for the gain of the complementary antenna. In the 15 dB bandwidth from 2.28 to 2.45 GHz, the antenna has a measured gain from 3.81 to 3.89 dBi and a simulated gain from 4.15 to 4.27 dBi. The error of the antenna gain between the simulation and measurement is between 0.34 and 0.38 dBi. This may be due to the difference in the material's dielectric constant during the antenna fabrication process and insufficient processing accuracy. Table 2 shows the comparison between the proposed antenna and the reference. The antenna has wider impedance bandwidth and higher front-to-back ratio characteristics.

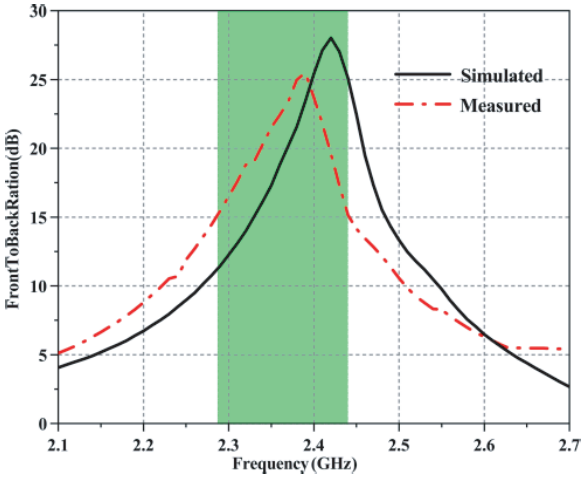

Figure 9. Simulated and measured front-to-back ratio.

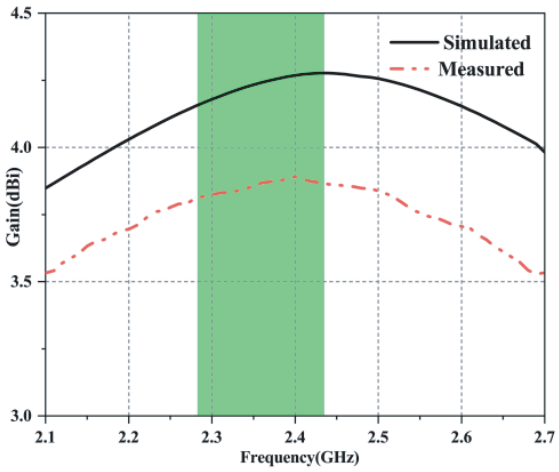

Figure 10. Simulated and measured gain.

Table 2. Performance comparison with other antennas in some literatures.

Ref. Ant.	Ant. Type	Impedance Bandwidth ($S_{11} < -10$ dB)	FTBR Bandwidth ($F/B > 15$ dB)	Peak FTBR (dB)	Gain (dBi)
[12]	ME-dipole antenna	2.73%	~	17.5	3.55
[14]	Magnetic dipole	10.5%	0	13.7	~
[15]	ME-dipole antenna	1.32%	0	13.3	5.4
[18]	ME-dipole antenna	13.3%	~	24.1	8.1
This work	ME-dipole antenna	48.05%	7.1%	25.4	3.89

4. CONCLUSION

A planar broadband end-fire antenna with a high front-to-back ratio has been investigated in this paper. The antenna is composed of a segmented loop and an electric dipole element. Wideband dipoles and parasitic magnetic loops improve the bandwidth and directivity of the antenna. A simple and low-cost antenna fabrication is shown. The proposed antenna is fabricated and measured. The prototype antenna has impedance bandwidth of 48.05% (1.66–2.71 GHz) for $|S_{11}| < -10$ dB, 15 dB front-to-back ratio bandwidth of 7.1% (2.28–2.45 GHz), and a maximum front-to-back ratio of 25.4 dB. Therefore, the antenna is very simple in structure and can be applied in a wireless communication system.

ACKNOWLEDGMENT

This work was supported in part by the Yunnan Provincial Foundation Program (202201AT070202) and the National Key Research and Development Program of China (2018YFB2200500).

REFERENCES

1. Haskou, A., A. Sharaiha, and S. Collardey, "Design of small parasitic loaded superdirective end-fire antenna arrays," *IEEE Transactions on Antennas and Propagation*, Vol. 63, No. 12, 1–1, 2015.
2. Lin, W. and R. W. Ziolkowski, "Electrically small, low-profile, huygens circularly polarized antenna," *IEEE Transactions on Antennas and Propagation*, Vol. 66, No. 2, 636–643, 2017.
3. Podilchak, S. K., A. P. Freundrofer, and Y. M. M. Antar, "Planar antenna for directive beam steering at end-fire using an array of surface-wave launchers," *Electronic Letter*, Vol. 45, No. 9, 444–445, 2009.
4. Juan, Y., W. Q. Che, Z. N. Chen, and W.n Yang, "A longitudinally compact Yagi-Uda antenna with a parasitic interdigital strip," *IEEE Antennas Wireless Propagation Letter*, Vol. 16, 2618–2621, 2017.
5. Yeo, J. and J. I. Lee, "Bandwidth enhancement of double-dipole quasi-yagi antenna using stepped slot-line structure," *IEEE Antennas Wireless Propagation Letter*, Vol. 15, 694–697, 2016.
6. Kaneda, N., W. R. Deal, Y. Qian, et al., "A broadband planar quasi-Yagi antenna," *IEEE Transactions on Antennas Propagation*, Vol. 50, No. 8, 1158–1160, 2002.
7. Li, Y., H. Xu, W. Wu, et al., "A non-balancing end-fire microstrip dipole with periodic-offset DSPSL substrate," *IEEE Transactions on Antennas Propagation*, Vol. 65, No. 5, 2661–2665, 2017.
8. Boyuan, M., J. Pan, S. D. Huang, et al., "Unidirectional dielectric resonator antennas employing electric and magnetic dipole moments," *IEEE Transactions on Antennas and Propagation*, Vol. 69, No. 10, 6918–6923, 2021.
9. Guo, L., K. W. Leung, and Y. M. Pan, "Compact unidirectional ringdielectric resonator antennas with lateral radiation," *IEEE Transactions on Antennas and Propagation*, Vol. 63, No. 12, 5334–5342, 2015.
10. Ouyang, J., Y. M. Pan, and S. Y. Zheng, "Center-fed unilateral and pattern reconfigurable planar antennas with slotted ground plane," *IEEE Transactions on Antennas and Propagation*, Vol. 66, No. 10, 5139–5149, 2018.
11. Zeng, J. and K. M. Luk, "Wideband millimeter-wave end-fire magnetoelectric dipole antenna with microstrip-line feed," *IEEE Transactions on Antennas and Propagation*, Vol. 68, No. 4, 2658–2665, 2020.
12. Tang, M. C., B. Zhou, and R. W. Ziolkowski, "Low-profile, electrically small, huygens source antenna with pattern-reconfigurability that covers the entire azimuthal plane," *IEEE Transactions on Antennas and Propagation*, Vol. 65, No. 99, 1063–1072, 2017.
13. Sun, K., Y. W. Zhao, Y. P. Chen, et al., "Improved HM-SIW cavity-cascaded array with high front-to-back ratio based on complementary element," *IEEE Transactions on Antennas and Propagation*, Vol. 68, No. 9, 6821–6825, 2020.
14. Yang, H. Q., M. You, W.-J. Lu, et al. "Envisioning an end-fire circularly polarized antenna: Presenting a planar antenna with a wide beamwidth and enhanced front-to-back ratio," *IEEE Antennas Propagation Magazine*, Vol. 60, No. 4, 70–79, 2018.
15. Wu, Z., M. C. Tang, M. Li, and R. W. Ziolkowski, "Ultralow-profile, electrically small, pattern-reconfigurable metamaterial inspired huygens dipole antenna," *IEEE Transactions on Antennas and Propagation*, Vol. 68, No. 3, 1238–1248, 2020.
16. Hu, P. F., Y. M. Pan, S. Zheng, and B. J. Hu, "The design of miniaturized planar endfire antenna with enhanced front-to-back ratio," *IEEE Transactions on Antennas and Propagation*, Vol. 68, No. 10, 7190–7195, 2020.
17. Wang, L., Y.-C. Jiao, and Z. Weng, "Novel dual-band circularly polarized planar endfire antenna with enhanced front-to-back ratios," *IEEE Transactions on Antennas and Propagation*, Vol. 70, No. 2, 969–976, 2022.
18. Yin, J. Y. and L. Zhang, "Design of a dual-polarized magnetoelectric dipole antenna with gain improvement at low elevation angle for a base station," *IEEE Antennas and Wireless Propagation Letters*, Vol. 19, No. 5, 756–760, 2020.

19. Best, S. R., "Progress in the design and realization of an electrically small Huygens source," *2010 International Workshop on Antenna Technology (iWAT)*, 2010.
20. Alitalo, P., A. O. Karilainen, T. Niemi, C. R. Simovski, et al., "A linearly polarized huygens source formed by two omega particles," *Proceedings of the 5th European Conference on Antennas and Propagation (EUCAP)*, 2302–2305, 2011.
21. Chlavin, A., "A new antenna feed having equal E- and H-plane patterns," *Transactions of the IRE Professional Group on Antennas and Propagation*, Vol. 2, No. 3, 113–119, 1954.
22. Chan, P. W., H. Wong, and E. K. N. Yung, "Unidirectional antenna composed of dipole and loop," *Electronics Letters*, Vol. 43, No. 22, 1176–1178, 2007.
23. Li, Z. R., L. D. Tan, X. L. Kang, J. X. Su, et al., "A novel wideband end-fire conformal antenna array mounted on a dielectric cone," *Applied Computational Electromagnetics Society Journal*, Vol. 31, No. 8, 933–942, 2016.
24. Balanis, C. A., *Antenna Theory: Analysis and Design*, John Wiley & Sons, New York, 2005.